Available online at www.sciencedirect.com
SCIENCE DIRECT
Cement and Concrete Research 36 (2006) 1176–1190
Cement and Concrete Research

Alteration of alkali reactive aggregates autoclaved in different alkali solutions and application to alkali–aggregate reaction in concrete (I) Alteration of alkali reactive aggregates in alkali solutions

Duyou Lu [a,b,*], Laibao Mei [a], Zhongzi Xu [a], Mingshu Tang [a], Benoit Fournier [b]

[a] College of Materials Science and Engineering, Nanjing University of Technology, 5 New Model Road, Nanjing, Jiangsu, 210009, China
[b] ICON/CANMET, Natural Resources Canada, 405 Rochester Street, Ottawa, ON, Canada, K1A 0G1

Received 11 November 2005; accepted 12 January 2006

Abstract

Surface alteration of typical aggregates with alkali–silica reactivity and alkali–carbonate reactivity, i.e. Spratt limestone (SL) and Pittsburg dolomitic limestone (PL), were studied by XRD and SEM/EDS after autoclaving in KOH, NaOH and LiOH solutions at 150 °C for 150 h. The results indicate that: (1) NaOH shows the strongest attack on both ASR and ACR aggregates, the weakest attack is with LiOH. For both aggregates autoclaved in different alkali media, the crystalline degree, morphology and distribution of products are quite different. More crystalline products are formed on rock surfaces in KOH than that in NaOH solution, while almost no amorphous product is formed in LiOH solution; (2) in addition to dedolomitization of PL in KOH, NaOH and LiOH solutions, cryptocrystalline quartz in PL involves in reaction with alkaline solution and forms typical alkali–silica product in NaOH and KOH solutions, but forms lithium silicate (Li_2SiO_3) in LiOH solution; (3) in addition to massive alkali–silica product formed in SL autoclaved in different alkaline solutions, a small amount of dolomite existing in SL may simultaneously dedolomitize and possibly contribute to expansion; (4) it is promising to use the duplex effect of LiOH on ASR and ACR to distinguish the alkali–silica reactivity and alkali–carbonate reactivity of aggregate when both ASR and ACR might coexist.

Keywords: Alkali–aggregate reaction; Alkali–silica reaction; Alkali–carbonate reaction; Microstructure; Lithium compounds

1. Introduction

1.1. Alkali in accelerated testing for alkali–aggregate reactivity

Enhanced alkali levels both in mortar or concrete specimens and in soak solution combined with elevated temperature have been widely used in order to identify the potential alkali reactivity of aggregates in the laboratory in a relatively short time. Enhanced alkali levels have usually been achieved by adding appropriate chemicals to the mortar or concrete mixture, or by storing the test specimens in alkali-bearing solutions. NaOH and KOH are commonly used for this purpose. The alkali levels used either in the test specimens or in solution, or in both, also varies from one study to another. For instance, Tang et al. [1] used KOH to enhance the alkali content of mixtures made with a low-alkali cement to 1.5% Na_2O equivalent and stored the specimens in a 10% KOH solution. Oberhoster and Davies [2] immersed their mortar bars in a 1 M NaOH to enhance alkali level. Chatterji [3] used saturated NaCl solution to accelerate ASR in the laboratory. Recently, Xu et al. [4,5] used KOH to increase the alkali content of low alkali–cement pastes to 1.5% Na_2O equivalent and cured the specimens in 1 M NaOH solution to test alkali–silica reactivity and alkali–carbonate reactivity of aggregate. The use of NaOH is specified in ASTM C1293 and CSA A 23.2–14 to adjust the cement alkali content to 1.25% Na_2O equivalent [6,7]. The adoption of NaOH or KOH to adjust

* Corresponding author. College of Materials Science and Engineering, Nanjing University of Technology, 5 New Model Road, Nanjing, Jiangsu, 210009, China. Tel.: +11 86 25 8358 7248; fax: +11 86 25 8358 7251.
E–mail addresses: duyoulu@njut.edu.cn, luduyou@yahoo.com (D. Lu).

0008-8846/$ - see front matter © 2006 Elsevier Ltd. All rights reserved.
doi:10.1016/j.cemconres.2006.01.008

the alkali content of cement or soak solution in testing method was mainly following the developer of the method. There is lack of systematic study to compare the effect of different chemicals on AAR and its expansion.

Total alkalis in cement and concrete are often expressed as Na_2O equivalent, in which K_2O is transferred to Na_2O using the multiplying factor 0.658, which is based on the ratio of their molecular weight, assuming sodium and potassium have the same effect. Generally, when limiting the alkali content to control AAR, much attention is paid to the total alkali content of cement or concrete. Little care is taken to whether Na_2O and K_2O have the same effect on AAR. If they really have different effect on AAR, in addition to the total alkali content, the species of alkali from different sources should also be considered.

1.2. LiOH and AAR

Since the pioneering work of McCoy and Caldwell in 1951 [8], the effectiveness of various lithium compounds, such as LiF, Li_2CO_3, $LiNO_3$, $LiOH{\cdot}H_2O$, in controlling ASR expansion has been evaluated by a number of researchers worldwide [9–18]. Globally, there is a minimum molar ratio ([Li]/[Na+K]) for lithium compounds to suppress ASR expansion, and this ratio varies with the type of lithium compound, concrete alkali content and the reactivity and composition of the reactive aggregate. Since there is no standard method for assessing effectiveness of lithium compounds and the methods and aggregates adopted by various researchers were different, the method used might also have influences on the minimum molar ratio of ([Li]/[Na+K]). Among lithium compounds, lithium nitrate is generally more efficient at reducing ASR expansion than other lithium compounds when used at similar molar ratios because it does not raise pore solution pH [19]. Compared with to lithium nitrate, a higher [Li/(Na+K)] molar ratio is necessary for LiOH to reduce expansion to similar levels; LiOH can also show a pessimum effect, where low and moderate amounts of LiOH can actually increase expansion. The pessimum effect of LiOH was attributed to an increase in the alkalinity of the pore solution that is triggered by the addition of LiOH [12,13]. Several studies have identified an apparent disconnect between aggregate reactivity and required lithium dosage to control expansion. Some extremely reactive aggregates respond very well to lithium, whereas other aggregates that are not as obviously reactive do not respond as well to lithium [18,19]. Although the reason for the disconnect is still not clear and the mechanisms by which lithium compounds suppress ASR expansion are not fully understood [19], it is widely accepted that lithium compounds, when used in sufficient quantity, can successfully suppress ASR expansion.

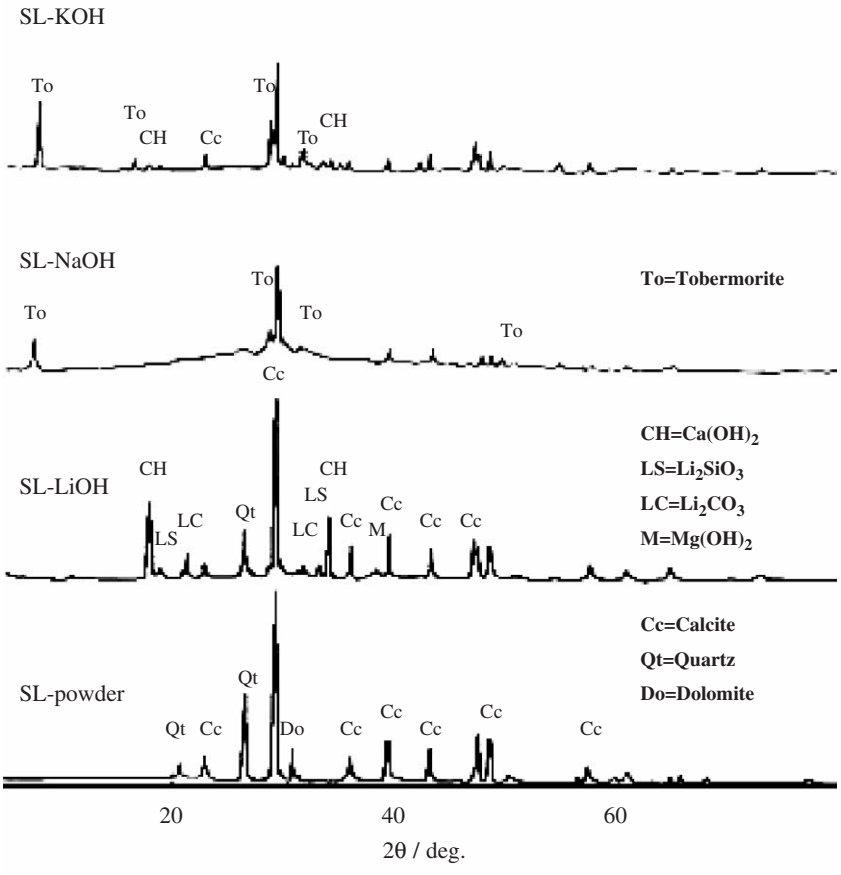

Fig. 1. XRD pattern of the surface of Spratt limestone after autoclaved in different alkali media.

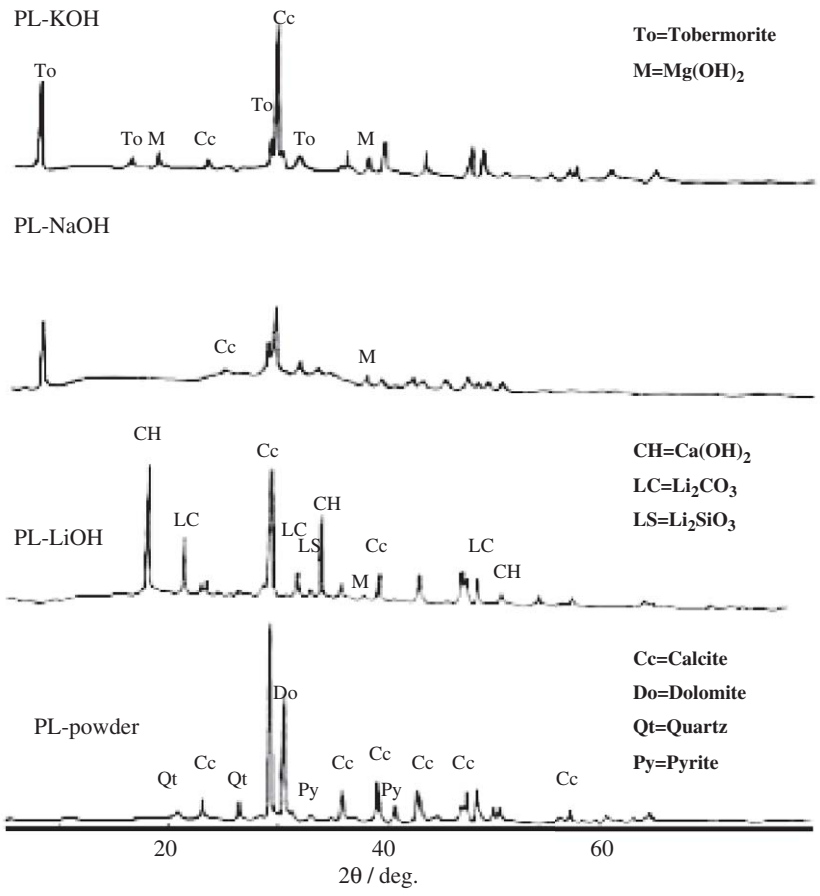

Fig. 2. XRD pattern of the surface of Pittsburg limestone after autoclaved in different alkali media.

Unfortunately, lithium compounds have shown to be less effective in controlling expansion due to alkali–carbonate reaction (ACR) [20]. The existence of dedolomitization reaction in lithium hydroxide, which suggests that lithium hydroxide can induce ACR, was detected by Wang and Gillott [21]. Qian et al. [22] confirmed the duplex effect of LiOH on ASR and ACR, i.e. it can suppress ASR and induce ACR, and verified the ACR, rather than ASR, was responsible for the expansion of the argillaceous dolomitic limestone with typical texture from Kingston, Ontario, Canada. However, some other argillaceous dolomitic limestone can exhibit both ASR and ACR [22,23]. It is common that dolomite-bearing carbonate rocks contain some microcrystalline or cryptocrystalline quartz [23–25], and the association with ASR is the main reason that the existence of deleterious ACR was doubted by some researchers [26]. ACR actually presents distinctive characteristics compared to ASR in

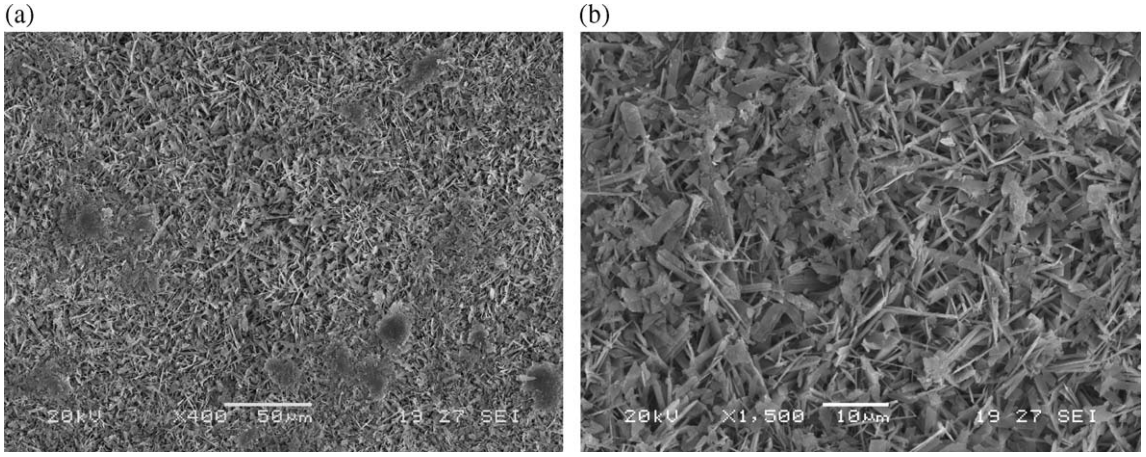

Fig. 3. SEM image of SL surface autoclaved at 150 °C in KOH for 150 h. (a) Loose arrangement of reaction product. (b) Lath-shaped crystals.

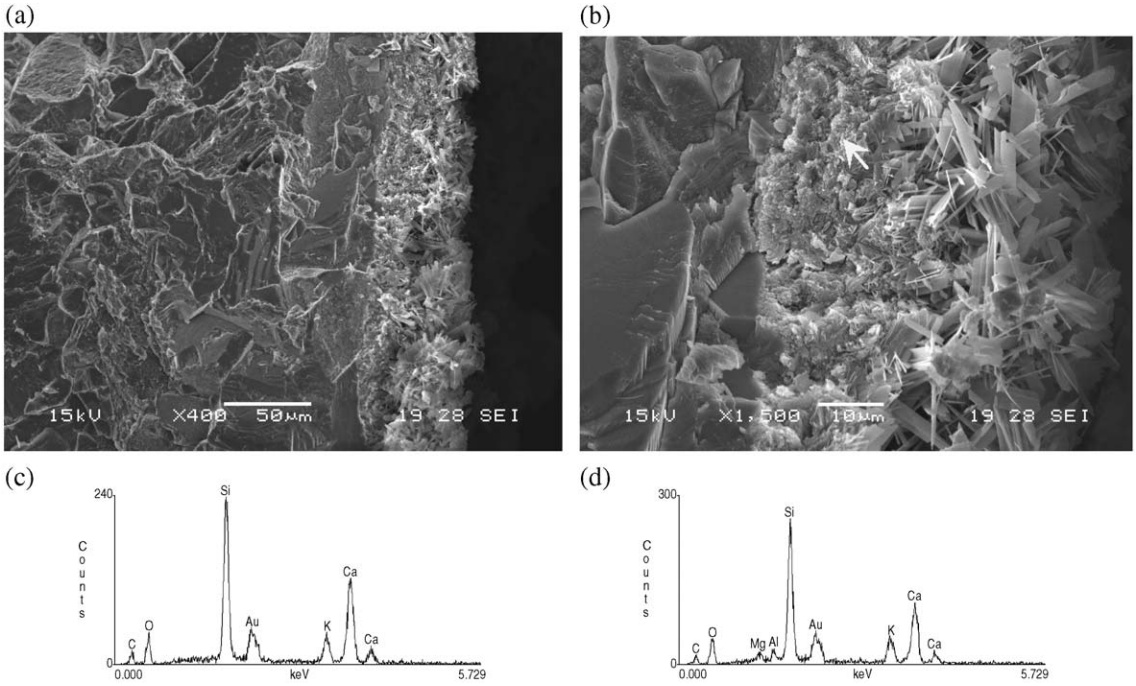

Fig. 4. SEM images of fractured surface of SL autoclaved at 150 °C in KOH for 150 h. (a) Layer of reaction product; (b) Enlargement of (a); (c) EDS spectrum of lath-shaped crystal; (d) EDS spectrum of gel-like product in transition layer, arrow indicates the position analyzed.

expansive process, mechanisms involved, as well as the resulting poor response to the preventive measures commonly used for ASR, such as SCMs and limiting concrete alkali content. Consequently, it is necessary for both academic and engineering practice to develop a method to distinguish ACR from ASR when ACR may coexist with ASR.

1.3. Scope of the work

Autoclave treatment on mortars or concrete prisms has been successfully used as ultra-accelerated test for assessment of alkali–aggregate reactivity or ASR risks of actual concrete compositions since the Chinese Autoclave Method for alkali–

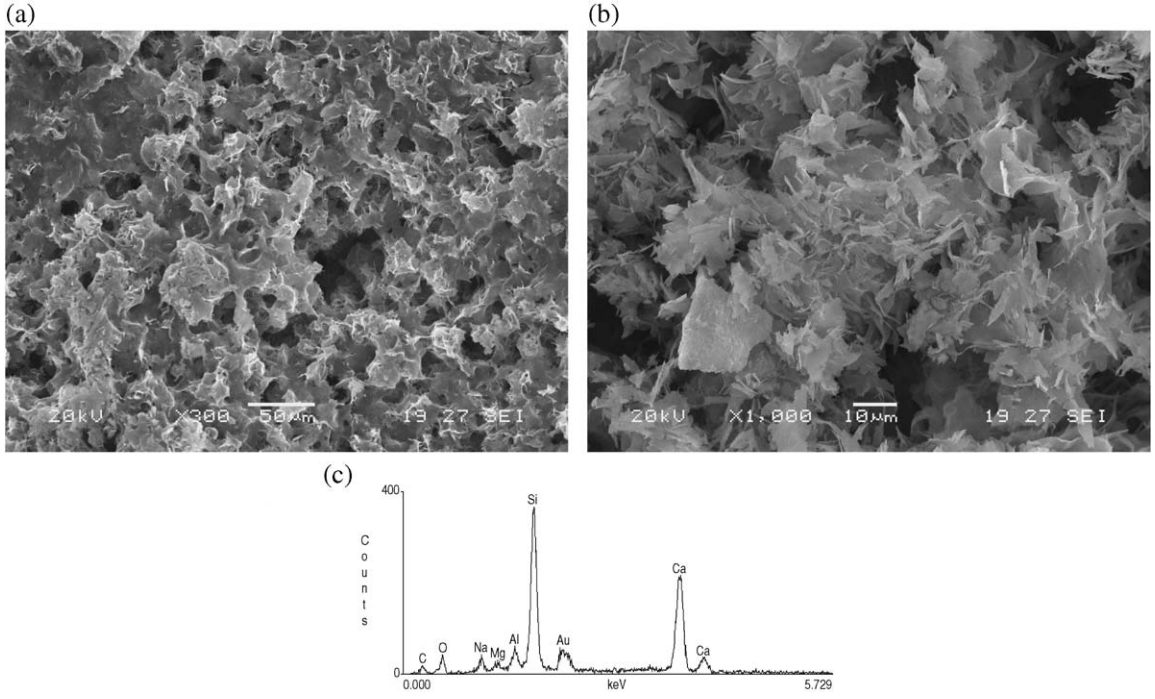

Fig. 5. SEM images of SL surface autoclaved at 150 °C in NaOH for 150 h. (a) Inhomogenouly deposited product. (b) Flaky semi-crystalline product; (c) EDS spectrum of product formed on surface.

silica reactivity of aggregate, which tests the mini mortar bar expansion in KOH solution at 150 °C, was proposed in 1983 [1,27–33]. Although the temperatures or specimen parameters varies from one study to another, globally, the autoclave results have satisfactory correlation with field records or with the results of concrete prism test conducted at 38 °C and over 95% R.H.

For developing accelerating testing method to classify ASR and ACR for dolomite-bearing aggregate, the effect of NaOH, KOH and LiOH on the expansion of typical alkali–silica reactive aggregates and alkali–carbonate reactive aggregate was studied by autoclaving concrete microbars in NaOH, KOH as well as LiOH solutions with the same molar concentration. Typical alkali–silica reactive aggregates and alkali–carbonate reactive aggregate were also autoclaved in corresponding alkali solutions. The present work is aimed at clarifying the effect of different alkalis on AAR and determining the possible reasons of the difference. This paper, as part one of the study, reports the alteration of alkali–reactive aggregates autoclaved in different alkali solutions.

2. Materials and experimental

2.1. Reactive aggregates

Two well-known alkali-reactive aggregates were used in this study. The Spratt limestone (SL) is a fine-grained siliceous limestone from the Spratt quarry near Ottawa, Canada. The reactive phase in the Spratt limestone is cryptocrystalline quartz disseminated in the matrix of calcite in the rock. Concrete structure deterioration associated with the use of this kind of aggregate has been reported in various region of eastern Canada [33,34]. The aggregate has commonly been used as a reference aggregate

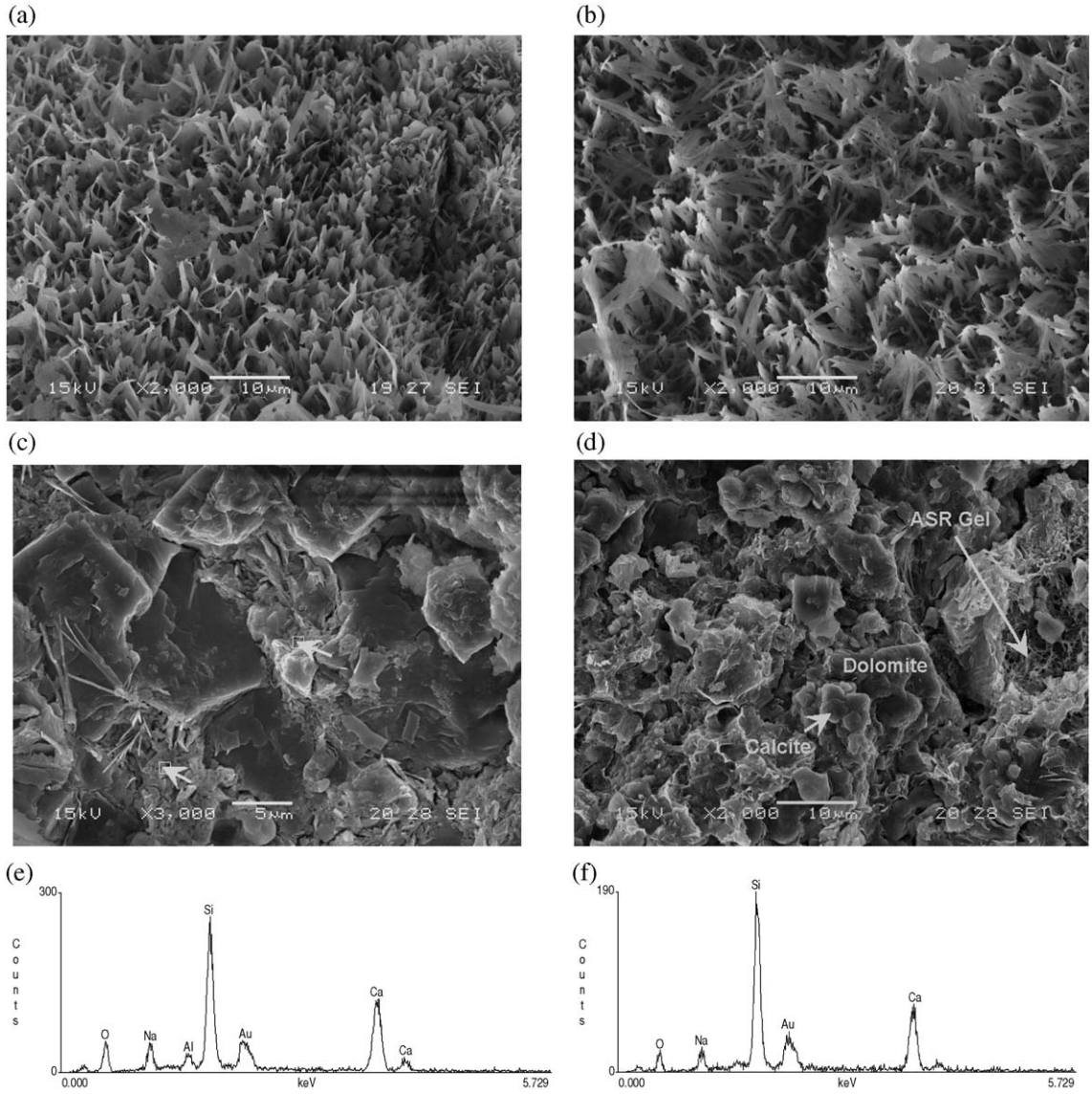

Fig. 6. SEM images taken inside of SL autoclaved at 150 °C in NaOH for 150 h. (a, b) Fibrous ASR product; (c) ASR gel formed between calcite grains; (d) Coexistence of ASR gel and reacted dolomite; (e) EDS spectrum of fibrous ASR products; (f) EDS spectrum of gel between calcite particles.

worldwide and generates high ASR expansion; it will also be used as reference ASR aggregate by RILEM committee TC ARP.

The second aggregate is an argillaceous dolomitic limestone (PL) from Pittsburg quarry, Kingston, Canada, which is a typical alkali–carbonate reactive rock and has caused concrete deterioration in Kingston area of Canada [34]. The rock consists of about 30% dolomite, 60% calcite and about 10% acid insoluble residue.

2.2. Experimental method

Three pieces of each aggregate, about 2 by 1 by 0.5 cm in size, were prepared with one polished surface. The pieces were respectively immersed in NaOH, KOH and LiOH solutions with the same concentration, i.e. 1.8 M, in stainless steel jar and autoclaved at 150 °C for up to 150 h. XRD was carried out on the polished surfaces after the alkali attack,

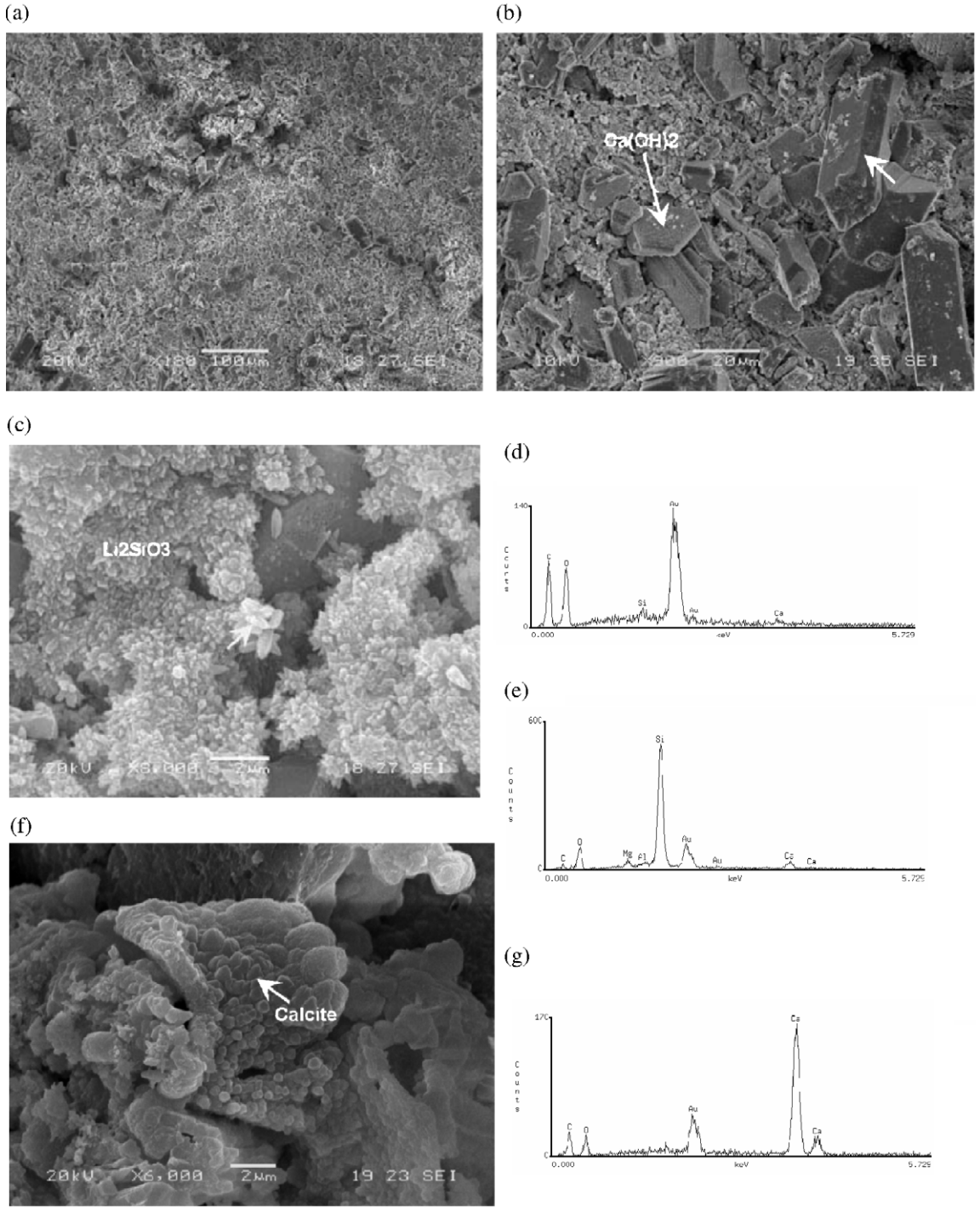

Fig. 7. SEM/EDS of products formed on the surface of SL autoclaved at 150 °C in LiOH for 150 h. (a) Overview of the surface; (b) Li_2CO_3, $Ca(OH)_2$ and Li_2SiO_3 formed on surface; (c) Enlargement of Li_2SiO_3; (d,e) EDS spectrums of Li_2CO_3 and Li_2SiO_3; (f,g) Newly formed calcite crystal and its EDS Spectrum. Arrows indicate positions analyzed.

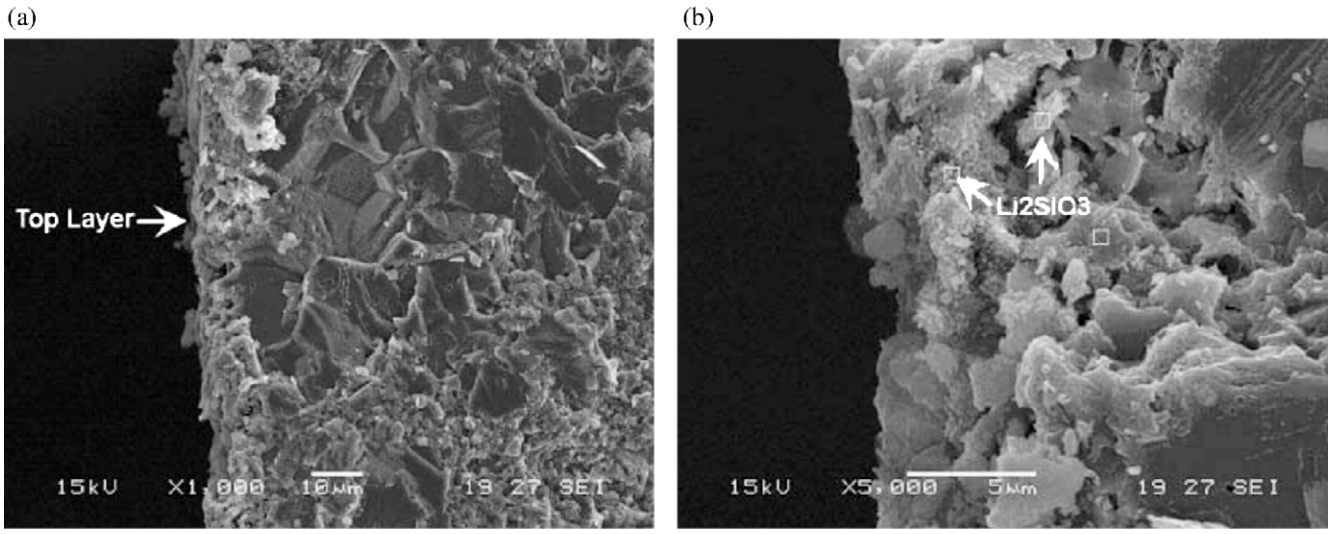

Fig. 8. SEM/EDS of fractured surface of autoclaved at 150 °C in LiOH for 150 h. (a) Product layer formed on polished surface; (b) Enlargement of the layer of product.

with the XRD pattern of untreated powder for comparison. SEM/EDS were used to examine the morphology and chemical composition of product formed on the surface in alkali solution. Fractured samples were also carefully prepared to observe the depth of product formation or alkali attack in each aggregate particle.

3. Experimental result

3.1. XRD result of SL autoclaved in alkali solution

Fig. 1 is the XRD pattern of the surface of SL autoclaved for 150 h in the different alkali solutions, with powder XRD pattern of untreated SL for comparison. The SL is essentially composed of calcite, quartz and a small amount of dolomite. After autoclaved in different alkali solution, the type and microtexture of the products formed on rock surface is quite different. In KOH solution, the products are tobermorite and calcium hydroxide. Only tobermorite was detected in NaOH solution, but the high background of the pattern (hump in the central portion of the X-ray diagram on Fig. 1 — SL NaOH) suggests amorphous product may also be formed. In LiOH solution, no tobermorite was detected, the products were mainly $Ca(OH)_2$, with a small amount of Li_2CO_3 and Li_2SiO_3.

In previous study [35], Li_2SiO_3 was also detected by XRD when silica glass particles were autoclaved in LiOH solution. It is worthy to note from Fig. 1 that quartz was evident in the powder X-ray diagram; but it was not detected after treated in the KOH and NaOH solutions and it was still there after treated in the LiOH solution. It suggested that quartz was dissolved in KOH and NaOH to form the tobermorite, but it was not dissolved so much in LiOH despite the high pH.

3.2. XRD result of PL autoclaved in alkali solution

Fig. 2 is the XRD pattern of the surface of PL autoclaved for 150 h in the different alkali solutions, with powder XRD pattern of untreated PL for comparison. The PL is essentially composed of calcite, dolomite with a small amount of quartz and pyrite. After autoclaved in the different alkali solutions, similar to SL, the type and microtexture of the products formed on rock surface is quite different. In KOH solution, the products are tobermorite and a small amount of $Mg(OH)_2$. In NaOH solution, tobermorite and $Mg(OH)_2$ were also detected, but with the high background of the pattern suggesting the product with low crystallinity formed. In LiOH solution, no tobermorite was detected, the products were mainly $Ca(OH)_2$, with a small amount of Li_2CO_3.

The source of silica for the formation of tobermorite for the PL might be from both quartz and clay minerals.

3.3. SEM/EDS study

3.3.1. SL in KOH solution

The micrographs of the polished and fractured surfaces of SL autoclaved in the 1.8 M KOH solution for 150 h are shown in

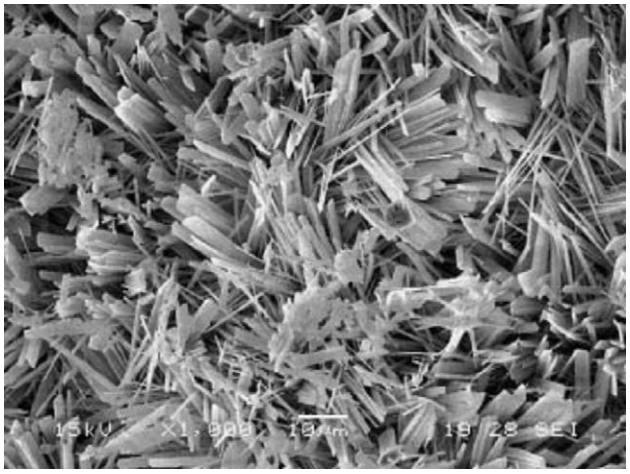

Fig. 9. Lath-shaped crystals formed on the surface of PL autoclaved at 150 °C in KOH for 150 h.

Figs. 3 and 4, respectively. The formation of product on the surface is not homogenous (Fig. 3a), and the product is mainly lath-shaped crystal, with a small amount of gel-like product (Fig. 3b). The lath-shaped crystals probably correspond to tobermorite identified by XRD. The thickness of the layer of products formed on the surface of the rock particles is about 50 μm, and the product can be clearly identified as two layers with different morphologies (Fig. 4). The top layer is mainly composed of a loose arrangement of lath-shaped crystals as shown in Fig. 3; the transition layer between the bulk rock particle and the top layer is mainly gel-like product. EDS results show that the lath-shaped crystals mainly consist of Si, Ca, K, while the gel-like product in transition layer consists a small amount of Mg and Al, in addition to Si, Ca, K. It indicated that the small amounts of clay minerals and dolomite in the rock might have involved in the reaction.

The gel-like product in the transition zone was relative dense, whereas the crystalline product on the top layer was

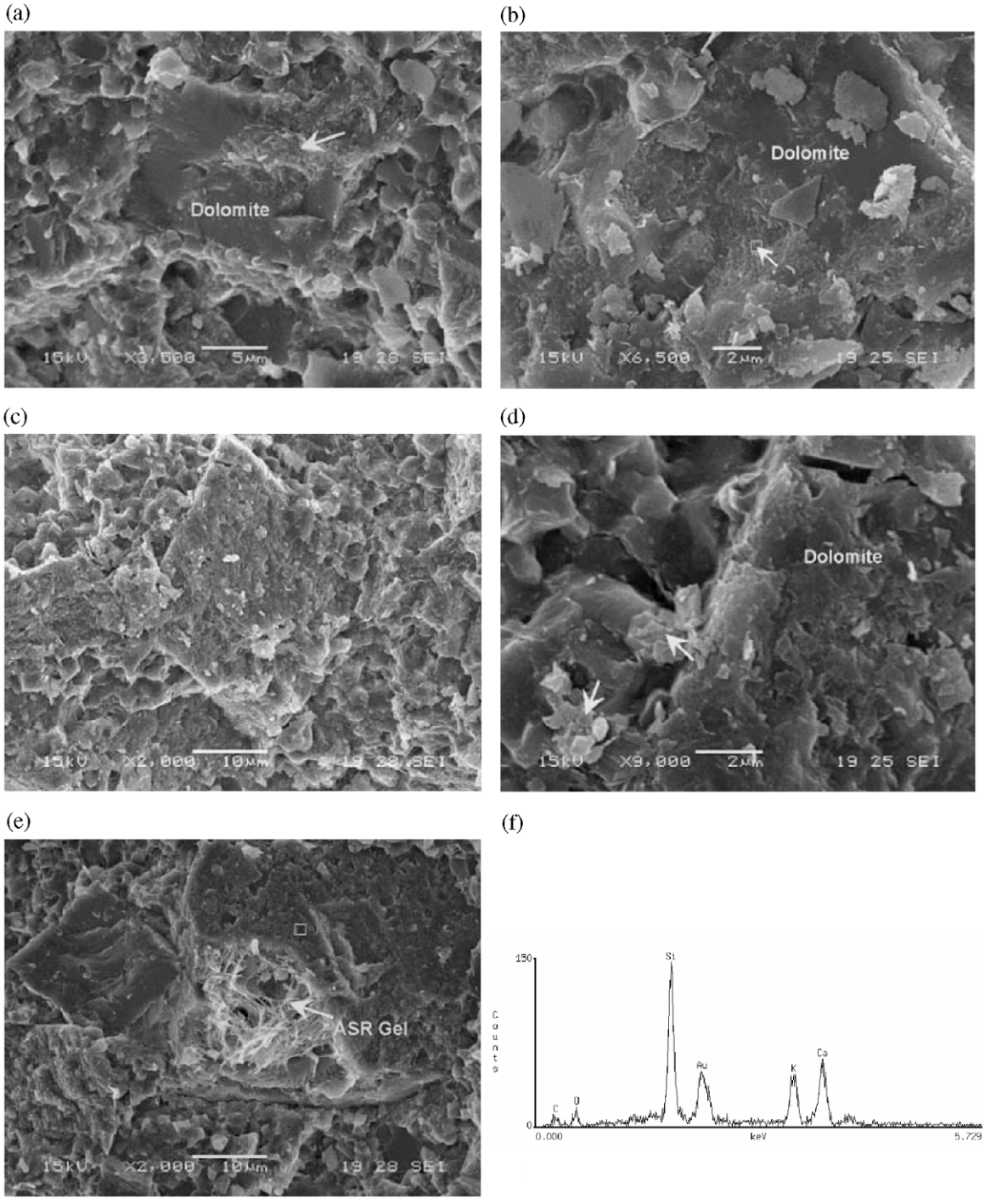

Fig. 10. SEM/EDS of fractured surface of PL autoclaved at 150 °C in KOH solution for 150 h. (a), (b) Corroded dolomite crystals; (c), (d) Corroded dolomite and product deposition beside dolomite; (e), (f) ASR gel formed in PL and its EDS spectrum.

quite loose and well-formed. Also, the size of the crystals at the interface between the gel and the crystalline product was relatively smaller compared with top layer crystals and it intergrew with gel. This suggests that, even under autoclave at 150 °C, the ASR product initially formed within the first thin layer of the particle is still gel, but the gel will/can transform to crystalline with the extension of the autoclave treatment time.

3.3.2. SL in NaOH solution

The rock piece was very fragile and almost disintegrated after the autoclave treatment in NaOH. Cracks in the specimen could easily be seen with naked eye. It was impossible to get a fractured surface like the specimen autoclaved in KOH solution because almost the whole particle had reacted to a significant extent.

Figs. 5 and 6 show selected SEM images taken from the surface and inside of the SL particle after autoclave treatment.

At low magnification, the surface was heterogeneous and looked highly porous with several holes of different sizes, which were due to the dissolution of silica into the solution (Fig. 5a). Some flaky semi-crystalline product shown in Fig. 5b can be observed at high magnification. The elemental composition of the flaky product detected by EDS was mainly Si, Ca, with small amounts of Al and Na. The flake product is probably the tobermorite corresponding to the XRD.

In addition to the flaky semi-crystalline product observed on the top surface, typical ASR products with different morphologies were also observed inside the reacted particle. Fig. 6a and b show bundles of blade- and needle-like sodium-rich products, respectively. Fibrous and amorphous gel products were also observed between calcite grains as shown in Fig. 6c and d. EDS patterns of these products with different morphologies were similar, as shown in Fig. 6e and f, but with a slightly lower aluminum content for the gel between calcite particles.

Interestingly, some reacted dolomite crystals were also observed in SL, with associated newly formed calcite particles thus suggesting that dedolomitization took place (Fig. 6d). It suggests that dolomite in SL might also have involved in reaction with NaOH solution and may have contributed to the cracking of SL through ACR.

3.3.3. SL in LiOH solution

Figs. 7 and 8 are SEM images of the top (polished) and fracture surfaces of the SL particle autoclaved in LiOH solution for 150 h.

As shown in Fig. 7a and b, on the surface of the specimen, large prismatic and hexagonal flake crystals, with size of about 20 μm, were disseminated or embedded in a layer of massive reaction products including large amounts of tiny particles. It can be noticed at high magnification that the tiny particles were agglomerates of smaller spindle crystals (Fig. 7c). From the XRD in Fig. 1 and the EDS patterns of the large prismatic crystals and agglomerates of tiny spindle crystals (Fig. 7d and e, respectively), the large prismatic crystals most likely correspond to Li_2CO_3 and the small spindle crystals to Li_2SiO_3 (lithium cannot be detected by EDS due to the lower energy of its X-ray photon). The larger hexagonal flakes are $Ca(OH)_2$ crystals.

Based on the SEM observations (e.g. Fig. 7), a layer of reaction products, which mainly consist of lithium silicate embedded with larger crystals of lithium carbonate and calcium hydroxide, can be formed around the SL rock particle when autoclaved in LiOH solution. As shown in Fig. 8a and b, the thickness of the product formed is about 10 μm, and the penetration of LiOH into the rock is not homogenous. The product layer is thicker than 20 μm at some interstices between calcite grains. It suggests that the lithium ion may penetrate into the rock through the interstices between the calcite grains forming the fine matrix of the rock.

3.3.4. PL in KOH solution

Figs. 9 and 10 show the SEM images of the top and fracture surfaces of PL autoclaved in KOH solution.

Similar to SL in KOH, the surface is covered with bundles of well-formed lath-shaped idiomorphic tobermorite crystals, but with a larger size (Fig. 9). Extensive microcracks can be easily seen on the fractured surface. Since the surface layer around the particle was very fragile following the autoclave treatment, it was not easy to determine the thickness of the product formed in the fractured surface. Sheet-like products were observed on the surface of some dolomite crystals. Interestingly, when the alkali hydroxides attack dolomite crystals, the dedolomitization is not only taking place at the interface between dolomite crystal and matrix, but also penetrates inside the dolomite crystals. Some typical SEM images of fractured surface are shown in Fig. 10. The product inside or near the dolomite is not always crystalline, gel-like product is also easily seen.

As expected, the cryptocrystalline quartz in PL, although in relatively small amounts, can be involved in the reaction with the KOH solution and form ASR gel that may also contribute to the cracking of rock. Fig. 10e and f shows the ASR gel formed inside the PL.

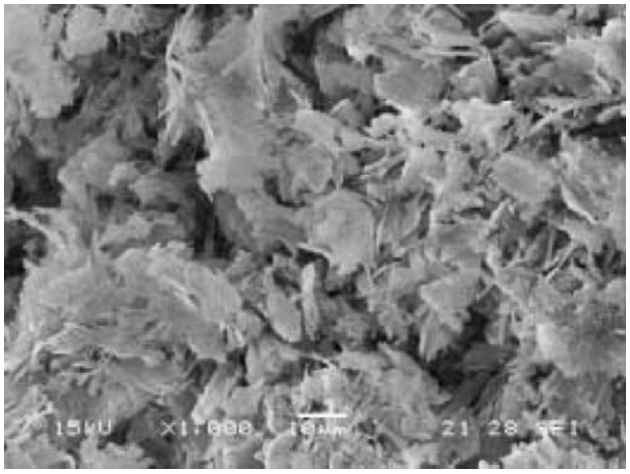

Fig. 11. Product formed on polished surface of PL autoclaved at 150 °C NaOH solution for 150 h.

3.3.5. PL in NaOH solution

The product formed on the polished surface of PL autoclaved in NaOH is mainly sheet-like product as shown in Fig. 11. The crystals were not so well-formed as that in KOH solution. The high background (hump in the central portion of the X-ray diagram on Fig. 2 — PL NaOH) of XRD spectrum in Fig. 2 indicates that some amorphous products have also formed. Same as SL in NaOH solution, the rock particle of PL was extensively cracked after the autoclave treatment and the surface layer was so fragile that it was difficult to prepare a fractured specimen to observe clearly the thickness of the product formed on the surface. Fig. 12 shows the selected SEM images of the fractured surface of PL. Fig. 12a indicates that two layers of product with distinct morphologies were formed on PL surface, although the bulk of the rock piece had also reacted. The outer layer (top layer), which was about 15 μm in thickness and was not clearly shown in picture, probably corresponds to a layer of sheet-like products as shown in Fig. 11. A lot of newly formed rhombic calcite crystals (recrystallined calcite),

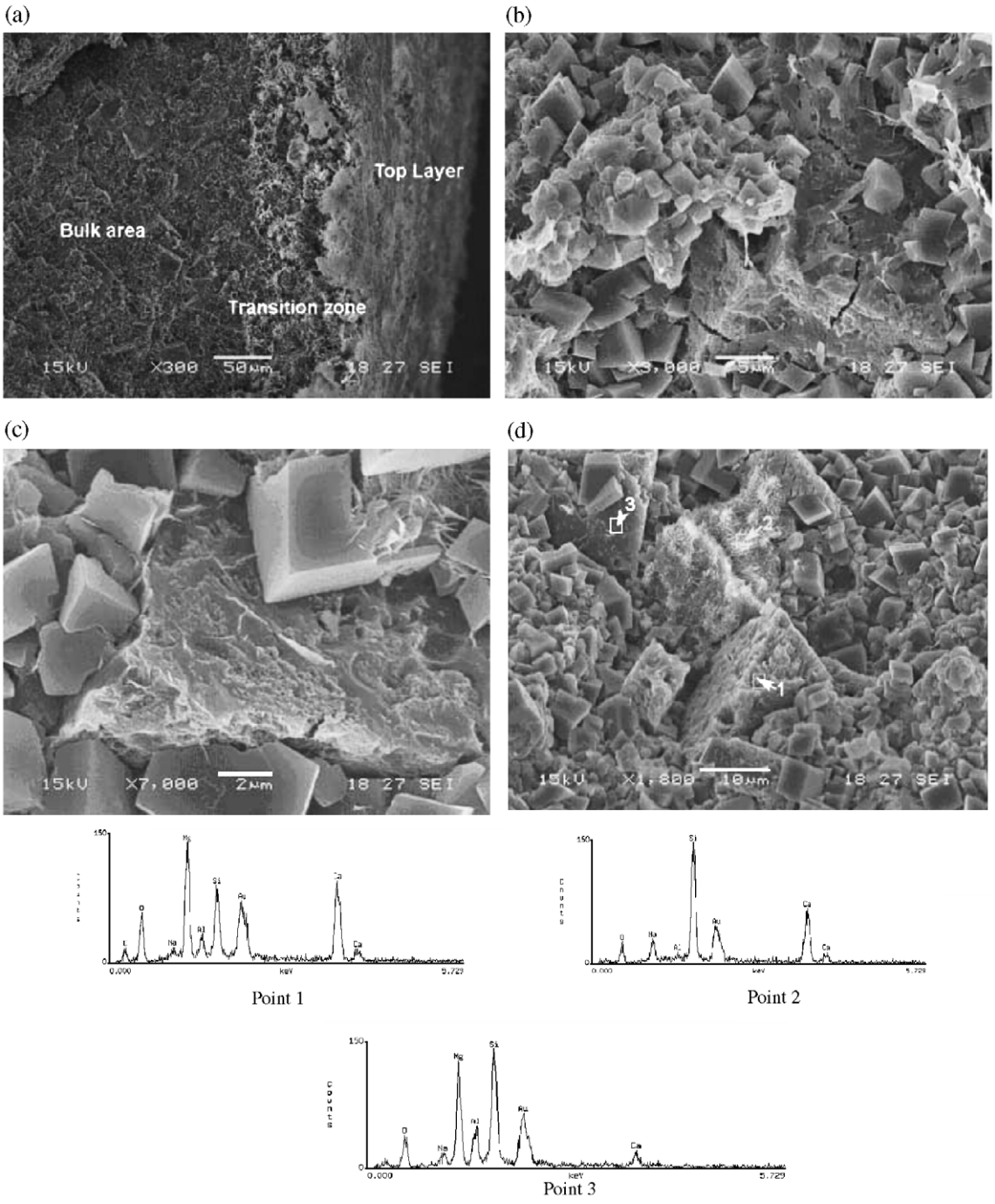

Fig. 12. Product formed on fractured surface of PL autoclaved at 150 °C in NaOH solution for 150 h. (a) Product layers; (b, c) Severely reacted dolomite; (d) Coexistence of fibrous ASR gel and dedolomitization; (e) EDS spectrums of positions shown in (d).

mixed with fibrous gel, were observed scattered both in the matrix of the particle and the transition zone, but with more gel in the transition zone. Some dolomite crystals were almost completely decomposed (Fig. 12b–d). The elemental compositions of the gel are Na, Si and Ca, typical ASR product composition. ASR may contribute to expansion to PL in NaOH.

Dolomite crystals had reacted significantly during the autoclave treatment in NaOH solution and a lot of perfect euhedral calcite crystals were formed inside PL. This is quite different from that in KOH solution. It may indicate that the dedolomitization process in NaOH and KOH are different at least in two aspects: the extent of dedolomitization process in NaOH is larger than that in KOH solution and the process is also different due to the different solubility of $Ca(OH)_2$ in these two solutions.

3.3.6. PL in LiOH solution

Figs. 13 and 14 show SEM images of the top and fractured surfaces of PL autoclaved in LiOH solution for 150 h.

Fig. 13 shows that the products formed on the surface mainly consist of prismatic crystals of Li_2CO_3 (even up to 50 μm in size) and hexagonal flakes of $Ca(OH)_2$ (over 10 μm). Small amounts of bundles of spindle Li_2SiO_3 crystals and hexagonal flakes of brucite with size of about 1 μm can also be observed at high magnification (Fig. 13c). Agglomerates of $Ca(OH)_2$ with clear cleavage are mainly near the bulk of the rock (Fig. 14a). $Mg(OH)_2$ besides dedolomitized dolomite crystal was also noticed.

The thickness of product formed on PL surface after the autoclave treatment in LiOH solution was about 30 μm (Fig. 14).

4. Discussion

4.1. Different attack of alkali hydroxides on alkali-reactive aggregates

The nature and thickness of the reaction products formed within the first layer of SL and PL are different after autoclaving in different alkali solutions. Well-formed crystalline reaction products were found on the surface of SL and PL particles in KOH and LiOH, although the gel might have initially formed on the SL surface, amorphous reaction products were mainly formed in NaOH solution. To some extent, the thickness of

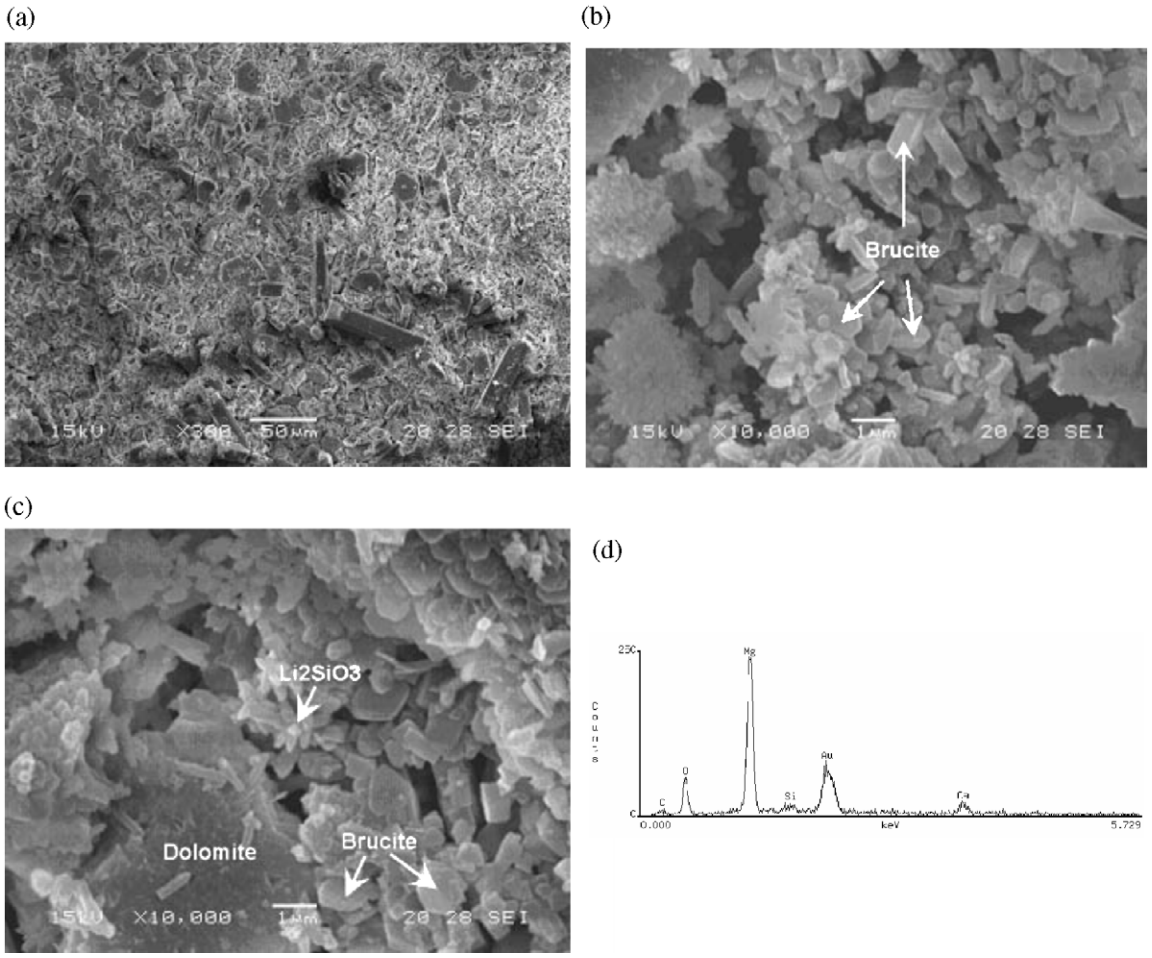

Fig. 13. Products formed on polished surface of PL autoclaved at 150 °C in LiOH solution for 150 h. (a) Overview of surface; (b) Hexagonal flaky $Mg(OH)_2$ crystal; (c) Li_2SiO_3 and $Mg(OH)_2$ crystals beside dolomite crystal; (d) EDS spectrum of hexagonal platy crystals shown in (b).

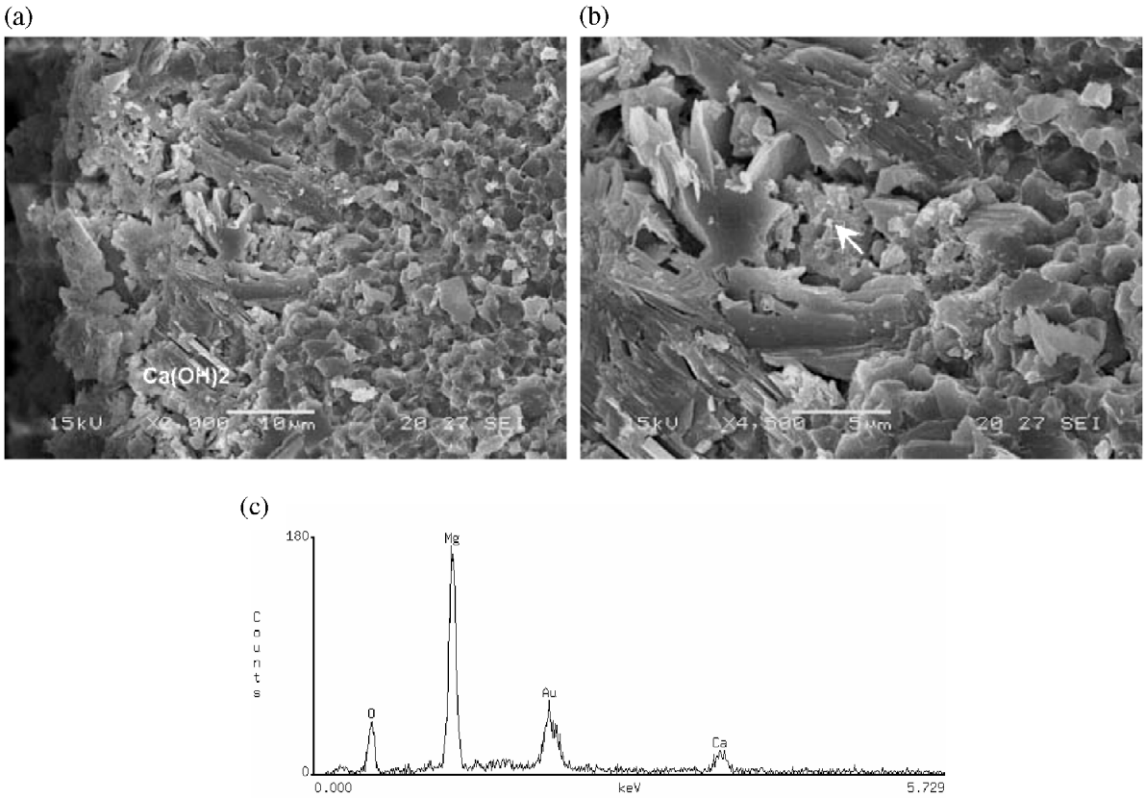

Fig. 14. Fractured surface of PL autoclaved at 150 °C in LiOH solution for 150 h. (a) Thickness of product; (b) Enlargement of Mg rich product; (c) EDS of Mg rich product.

products formed at the surface of the rock particles after the autoclave treatment can reflect the extent of the attack on aggregates by the different alkali solutions. After autoclaving in NaOH solution for 150 h, the bulk of two rock pieces were almost completely affected, thus clearly showing that, under the conditions used, NaOH had the strongest attack on the aggregate particles. The weakest attack was with LiOH solution, the thickness of products formed on SL and PL were 10 and 30 μm, respectively.

Comparing the amount of $Ca(OH)_2$ formed in the different alkali solutions, both SL and PL in LiOH gave the highest $Ca(OH)_2$ content, whereas there was few detectable $Ca(OH)_2$ deposited in KOH and NaOH solution. Garcia et al. [36] found that there are no significant differences in the dedolomitization mechanism involving NaOH or KOH solutions of low concentrations; however, for alkali–hydroxides solutions of concentrations higher than 0.6 M, the dedolomitization starts to show different behaviors at room temperature, with portlandite being saturated for KOH and unsaturated for NaOH. Since the solubility of portlandite decreases with increasing temperature, portlandite should be easy to be over saturated in 1.8 M LiOH and KOH at 150 °C, however, no $Ca(OH)_2$ was detected either in KOH or NaOH solution with 1.8 M. This may be largely due to the formation of tobermorite, which keeps $Ca(OH)_2$ being unsaturated in the solutions.

In examining the effect of various alkali-hydroxides on the dissolution rate of silica, Lawrence and Vivian [9] found that the dissolution rate increased in the following order: LiOH<-NaOH<KOH. Over time, however, the concentration of dissolved silica for each alkali–hydroxide approached the same value, independent of the alkali type; this suggests that the various alkali–hydroxides only influence the rate of dissolution of silica but not the extent of the solubility of silica. Wijnen et al. [37] found that the rate of silica dissolution decreased in a similar order and proposed that this rate decreases with increasing hydrated ion radius of the alkali metal cations in solution surrounding a silicate surface. Considering lithium, sodium and potassium, the rate of silica dissolution would, then, be the slowest in the presence of lithium, which has a larger hydrated ion radius than sodium which, in turn, has a larger hydrated ion radius than potassium.

However, in the presence of calcium and/or magnesium and under autoclave, the extent of the chemical reactions between silica and the alkali hydroxide solutions may be different and complicated due to the different solubility of $Ca(OH)_2$ and possibly different behaviors of tobermorite in such solutions. Both SL and PL contain large amounts of fine-grained calcite but largely different amounts of dolomite, both of which are unstable in alkali media [38]; these minerals can provide calcium ions for the formation of tobermorite, or portlandite during alkali attack. Dolomite can also provide magnesium for the formation brucite. Since portlandite has different solubility in different alkali hydroxide solutions, it was over saturated in the LiOH solution and remained subsaturated in the NaOH solution. In the KOH solution, brucite was observed on the

surface of PL, while portlandite was detected by XRD on the SL surface (Fig. 1). Although the dissolution rate of silica in KOH is higher than that in NaOH, NaOH showed higher degree of attack on SL and PL due to the lack of portlandite or brucite formation on the surface of SL and PL in NaOH solution. It also suggested that the formation of product layer around aggregate particle was important for preventing aggregate from further attack.

Also, the alkali hydroxide attack seems to vary from one aggregate to another. It is not easy to compare the effect of NaOH on SL and PL because almost the whole rock pieces were suffered severely corrosion. However, both KOH and LiOH solutions showed a relatively stronger attack on PL than that on SL. Stronger attack may lead to faster reaction and development of expansion, which might be one of the reasons why ACR develops faster than ASR in the field concrete in addition to the difference in the mechanisms involved in the two reactions.

4.2. Dedolomitization of PL in different alkali solution

Dedolomitization of dolomite crystals in PL was detected in LiOH, NaOH and KOH. Although Garcia et al. [36] found no significant differences in the dedolomitization mechanism between NaOH and KOH solutions of low-alkali concentration, regardless the process, the crystalline degree, morphology, and distribution of products are quite different when autoclaved in different alkali solutions with high concentration.

Comparing PL in KOH and NaOH solution, in addition to the formation of poorly crystalline and amorphous products in NaOH solution, a large amount of recrystallized calcite were found in the matrix of PL. Choquette et al. [38] found that, even at low temperature in 1 M NaOH, after 28 days, calcite crystals can be strongly corroded without precipitation. The experimental condition in this work, i.e. autoclave in 1.8 M NaOH solution at 150 °C for 150 h, was so severe that, in addition to dedolomitization of the dolomite crystals, the micrite matrix in PL was probably also unstable and experienced a dissolution and recrystallization process. On the other hand, high degree of dedolomitization may play an important role in contributing to the concentration of CO_3^{2-} to accelerate the process, because almost no such rhombic calcite crystals were found in PL autoclaved in KOH solution and SL autoclaved in NaOH, although dedolomitization may have taken place in both situations.

As Qian et al. stated [22], since Li_2CO_3 has a lower solubility than Na_2CO_3 and K_2CO_3, it will deposit in dedolomitization process in LiOH. Thus, dedolomitization in LiOH is a process with volume increase in solid phases, which is different from the solid phases volume-decreasing processes in NaOH and KOH. The expansion accompanying the dedolomitization in LiOH solution may be contributed from two aspects: the crystalline pressure due to the growth and rearrangement of dedolomitization products and the solid volume increase of the products.

It was also noted that dedolomitization of dolomite crystals is not limited to the surface of the dolomite crystals or at the interface between dolomite crystal and around the matrix, as shown in Fig. 10, it may also take place inside dolomite crystals.

ASR gel was observed inside PL specimens autoclaved in both NaOH and KOH, although very little gel was observed when autoclaved in KOH. ASR of the cryptocrystalline quartz in PL may contribute to the total expansion in such a severe condition. However, crystals of Li_2SiO_3 were formed in PL when autoclaved in LiOH. This suggests that the ASR from PL can be suppressed and has no contribution to the PL expansion in LiOH.

4.3. Possible contribution from ACR to expansion of SL

The possible contribution of ASR to the expansion process of some alkali–carbonate reactive dolomite-bearing aggregates has been noted by some researchers [22,23,26]. However, little attention was paid to the possible contribution from ACR to the ASR expansion of dolomite-bearing siliceous limestone. From above results on SL, dedolomitization seems to have occurred when it was autoclaved in alkaline solutions, especially in NaOH solution (Fig. 2, $Mg(OH)_2$ was detected when SL autoclaved in LiOH and Fig. 10d). Therefore, for some dolomite-bearing siliceous limestone showing typical alkali–silica reactivity, such as SL, dedolomitization of small amount of dolomite may also contribute to the total expansion, i.e. some siliceous limestone with small amount of dolomite may simultaneously contain an extent of alkali–carbonate reactivity, although it mainly exhibits alkali–silica reactivity. Since expansion from aggregate with alkali–silica reactivity can be suppressed by sufficient LiOH [18,19,22], and the dedolomitization can take place in LiOH solution, it is promising to use LiOH to distinguish the ACR contribution in dolomite-bearing siliceous aggregates.

5. Conclusions

(1) Compared to KOH and LiOH solutions with the same molar concentration, NaOH has the strongest attack on both alkali–silica and alkali–carbonate reactive aggregates under autoclave at 150 °C, while the weakest attack was with LiOH. For both aggregates, the microtexture, morphology and distribution of products formed in the different alkali solutions are quite different. More crystalline products are formed on rock surfaces in KOH than in NaOH solution, while almost no amorphous product formed in LiOH solution.

(2) The ASR product initially formed in NaOH and KOH under autoclave was ASR gel, but with the prolonging of autoclave time, it may transform to crystalline.

(3) In addition to dedolomitization of PL in KOH, NaOH and LiOH solutions, cryptocrystalline quartz in PL involved in reaction with alkaline and formed typical alkali–silica product in NaOH and KOH solutions, but formed lithium silicate (Li_2SiO_3) in LiOH solution.

(4) In addition to massive alkali–silica product formed in SL autoclaved in different alkaline solutions, small

amount of dolomite existed in SL may also simultaneously dedolomitize and possibly contribute to expansion of SL.

(5) It is promising to use the duplex effect of LiOH on ASR and ACR to distinguish the alkali–silica reactivity and alkali–carbonate reactivity of aggregate when both ASR and ACR might coexist. However, in LiOH solution, the products formed on surface of ASR aggregates were mainly crystalline under autoclave conditions, which might be different from that formed at lower temperature, especially in crystalline degree, it needs further study to compare the behavior of lithium on ASR at various temperatures.

Acknowledgements

This study was supported by National 973 key project of China, 2001CB610706 and Natural Science Fund from Jiangsu Provincial Department of Education, 05KJB430046. Thanks also to Dr. Paddy Grattan-Bellew from National Research Council of Canada for his help and suggestions in editing the draft of the paper.

References

[1] M.S. Tang, S.F. Han, S.H. Zheng, A rapid method for identification of reactivity of aggregate, Cement and Concrete Research 13 (1983) 417–422.

[2] R.E. Oberholster, G. Davis, An accelerated method for testing the potential alkali reactivity of siliceous aggregates, Cement and Concrete Research 16 (1986) 181–189.

[3] S. Chatterji, An accelerated method for the detection of alkali–aggregate reactivity of aggregates, Cement and Concrete Research 8 (1978) 647–649.

[4] Z.Z. Xu, Y. Shen, D. Lu, et al., Parameters for the New Chinese accelerated mortar bar testing for alkali–silica reactivity of aggregates, Journal of the University of Chemical Technology 20 (1998) 1–8.

[5] Z.Z. Xu, Xianghui Lan, Min Deng, Mingshu Tang, A new accelerated method for determining the potential alkali–carbonate reactivity, Proceedings of the 11th International Conference on Alkali–Aggregate Reaction, Quebec, 2000, pp. 129–138.

[6] ASTM C 1293, Standard Test Method for Concrete Aggregate by Determination of Length Change of Concrete Due to Alkali–Silica Reaction, Annual Book of ASTM Standards. Concrete and Aggregates, vol. 04-02, American Society for Testing and Materials, Philadelphia, U.S.A, 1996, pp. 648–653.

[7] CSA, A23.2-14A, Potentially expansibility of aggregates (Procedure for length change due to Alkali–Aggregate Reaction in concrete prisms), A23.1-11/A23.2-00 Concrete Materials and Methods of Concrete Construction/Methods of Testing for Concrete, CSA International, 2000, pp. 207–216.

[8] W.J. McCoy, A.G. Caldwell, New approach to inhibiting alkali–aggregate expansion, Journal of the American Concrete Institute 1951, 22 (9) (1951) 693–706.

[9] M. Lawrence, H.F. Vivian, The reactions of various alkalis with silica, Australian Journal of Applied Science 12 (1961) 96–103.

[10] Y. Sakaguchi, M. Takakura, A. Kitagawa, H. Takahiro, F. Tomosawa, A. Michihiko, The inhibition effect of lithium compounds on alkali–silica reaction, in: K. Okada, et al., (Eds.), Proceedings of the 8th International Conference on Alkali–Aggregate Reaction, Kyoto, Japan, 1989, pp. 229–234.

[11] Y. Ohama, K. Demura, M. Kakegawa, Inhibiting alkali–aggregate reaction with chemical admixtures, in: K. Okada, et al., (Eds.), Proceedings of the 8th International Conference on Alkali–Aggregate Reaction, Kyoto, Japan, 1989, pp. 253–258.

[12] D.C. Stark, Lithium admixtures — an alternative method to prevent expansive alkali–silica reactivity, Proceedings of 9th International Conference on Alkali–Aggregate Reaction. Concrete Society, vol. 2, London, UK, 1992, pp. 1017–1025.

[13] S. Diamond, S. Ong, The mechanisms of lithium effects on ASR, Proceedings of 9th International Conference on Alkali–Aggregate Reaction. Concrete Society, vol. 1, London, UK, 1992, pp. 269–278.

[14] J.S. Lumley, ASR suppression by lithium compounds, Cement and Concrete Research 27 (1997) 235–244.

[15] B.Q. Blackwell, M.D.A. Thomas, A. Sutherland, Use of lithium to control expansion due to alkali–silica reaction in concrete containing U.K. aggregates, in: V.M. Mahotra (Ed.), Proceedings of 4th International Conference on Durability of Concrete. ACI SP-170, American Concrete Institute, Detroit, 1997, pp. 649–663.

[16] M.D.A. Thomas, R. Hooper, D. Stokes, Use of lithium-containing compounds to control expansion in concrete due to alkali–silica reaction, Proceedings of the 11th International Conference on Alkali–Aggregate Reaction (ICAAR), Quebec, Canada, 2000, pp. 783–810.

[17] B. Durand, More results about the use of lithium salts and mineral admixtures to inhibit ASR in concrete, Proceedings of the 11th International Conference on Alkali–Aggregate Reaction (ICAAR), Quebec, Canada, 2000, pp. 623–632.

[18] B. Fournier, D.B. Stokes, A. Ferro, Comparative field and laboratory investigations on the use of supplementary cementing materials (SCMs) and lithium-based admixtures to control expansion due to alkali–silica reaction (ASR) in concrete, Proceedings of the 6th International CANMET/ACI Conference on Durability of Concrete, 2003, pp. 823–851, Thessaloniki, Greece.

[19] K.J. Folliard, M.D.A. Thomas, K.E. Kurtis, Guidelines for the Use of Lithium to Mitigate or Prevent ASR, 2003, Publication No. FHWA-RD-03-047, 61 pp.

[20] E.G. Swenson, J.E. Gillott, Characteristics of Kingston carbonate rock reactions, Highway Research Board, Bulletin 275 (1960) 18–31.

[21] H. Wang, J.E. Gillott, Alkali–carbonate reaction: significance of chemical and mineral admixtures, Magazine of Concrete Research 47 (1995) 69–75.

[22] Guangren Qian, Min Deng, Mingshu Tang, Expansion of siliceous and dolomitic aggregates in lithium hydroxide solution, Cement and Concrete Research 32 (2002) 763–768.

[23] Liang Tong, Mingshu Tang, Concurrence of alkali–silica and alkali–dolomite reaction, Proceedings of 10th International Conference on Alkali–Aggregate Reaction in Concrete, CSIRO, Melbourne, 1996, pp. 742–749.

[24] B. Fournier, M.-A. Berube, Alkali-reactivity potential of carbonate rocks from the St. Lawrence lowland, Quebec, Canada, Proceedings of 8th International Conference on Alkali–Aggregate Reaction in Concrete, Kyoto, Japan, 1989, pp. 363–368.

[25] B. Fournier, M.-A. Berube, Evaluation of a modified chemical method to determine the alkali reactivity potential of siliceous carbonate aggregates, in: C.A. Rogers (Ed.), Proceedings: Canadian Developments in Testing Concrete Aggregate for Alkali–Aggregate Reactivity, Ministry of Transportation, Ontario, 1990, pp. 118–135 (Report EM-92).

[26] T. Katayama, Critical review of carbonate reactions — is their reactivity useful or harmful, Proceedings of 9th International Conference on Alkali–Aggregate Reaction, vol. 1, Concrete Society, London, UK, 1992, pp. 508–517.

[27] A. Criaud, C. Vernet, C. Defosse, The microbar method, an accelerated expansion test for evaluating aggregates — assessment of Canadian aggregates, Canadian Developments in Testing Concrete Aggregates for Alkali–Aggregate Reactivity. Engineering Materials Report, vol. 92, Ministry of Transportation, Ontario, 1990, pp. 201–214.

[28] M.S. Tang, X.H. Lan, S.F. Han, Autoclave method for identification of alkali reactivity of carbonate rocks, Cement, Concrete and Composities 16 (1994) 163–167.

[29] A. Criaud, C. Vernet, C. Defosse, An accelerated method for the evaluation of ASR risks of actual concrete compositions, in: V.M. Marhotra (Ed.), Proceedings of the third CANMET/ACI International Conference on Durability of Concrete, Nice, France, 1994, pp. 687–712.

[30] M. Berra, T. Mangialardi, A.E. Paolini, Use of an ultra-accelerated concrete prism expansion test for alkali–silica reactivity assessment, Magazine of Concrete Research 57 (2005) 39–48.
[31] JIS A 1804, Methods of Test for Production Control of Concrete — Method of Rapid Test for Identification of Alkali Reactivity of Aggregate, 2001.
[32] M.A. Berube, B. Fournier, N. Dupont, P. Mongeau, J. Frenette, A simple autoclave mortar bar method for assessing potential alkali–aggregate reactivity in concrete, Proceedings of the 9th International Conference on Alkali–Aggreagte Reaction on Concrete, London, U.K., 1992, pp. 81–91.
[33] M.-A. Berube, B. Durand, D. Vezina, B. Fournier, Alkali–aggregate reactivity in Qubec(Canada), Canadian Journal of Civil Engineering 27 (2000) 226–245.
[34] C.A. Rogers, P.E. Grattan-Bellew, R.D. Hooton, J. Ryell, M.D.A. Thomas, Alkali aggregate reactions in Ontario, Canadian Journal of Civil Engineering 27 (2000) 246–260.
[35] Mo Xiangyin, Long-term effectiveness and mechanism of chemical admixtures in inhibiting Alkali–silica reaction, Ph D thesis, 2001, Nanjing University of Technology.
[36] E. Garcia, P. Alfonso, M. Labrador, S. Gali, Dedolomitization in different alkaline media: application to Portland cement paste, Cement and Concrete Research 33 (2003) 1443–1448.
[37] P.W.J.G. Wijnen, T.P.M. Beelen, J.W. de Haan, C.P.J. Rummens, L.J.M. van de Ven, R.A. van Santen, Silica gel dissolution in aqueous alkali metal hydroxides studies by 29Si NMR, Journal of Non-Crystalline Solids 109 (1989) 85–94.
[38] M. Choquette, M.-A. Berube, J. Locat, Behavior of common rock-forming minerals in a strongly basic NaOH solution, Canadian Mineralogist 29 (1991) 163–173.